Journal Name

ARTICLE

Synthesis of distorted nanographenes containing seven- and eight-membered carbocycles

Received 00th January 20xx,
Accepted 00th January 20xx

DOI: 10.1039/x0xx00000x

www.rsc.org/

Irene R. Márquez,†[a] Silvia Castro-Fernández,†[a] Alba Millán[a] and Araceli G. Campaña*[a]

This feature article focuses on the bottom-up approaches (solution-phase) based on organic synthesis for the preparation of saddle-shaped distorted polycyclic aromatic hydrocarbons (PAHs). We summarise the recent progress on the synthetic strategies followed to obtain well-defined nanographenes containing heptagonal and octagonal carbocycles, highlighting the novel strategy developed by our group together with our recent contributions in the area of distorted aromatics. The presence of seven- or eight-membered rings induces a saddle-shape curvature in the planar network pushing the structure out of the plane which influences the physical properties exhibited. Some brief details into the optical and electronic properties of those curved nanostructures are also discussed.

1. Introduction

The outstanding properties associated to graphene (*i.e.* a strong electric and thermal conductor and an elastic material) refer to pristine samples without structural defects. However, those defects have been observed in the graphene basic hexagonal network and can significantly modify its properties.[1] New useful semiconductor materials may arise from the controlled deviation of perfection and distorted materials could be useful for new applications in electronics and photonics. Among the defects observed in single-layer graphene, vacancies involve one or two atoms missing in the lattice. As consequence, sets of five and seven-membered rings and occasionally eight or nine-membered rings are typically observed in graphene samples.[2]

Polycyclic aromatic hydrocarbons (PAHs) or nanographenes have received significant attention as well-defined graphene fragments.[3] Nanographenes containing non-hexagonal rings or heteroatoms can be envisioned as ideal models of defective graphene. Therefore they might serve to experimentally corroborate the theoretical studies on the influence of topological defects in graphene structures. Those theoretical data indicated that the distortion from planarity caused by the presence of odd-member rings deeply influences the physical properties exhibited by those carbon nanostructures.[4]

Over the last two decades, extensive series of purely hexagonal atomically precise PAHs have been successfully synthesized in a well-defined manner by bottom-up synthetic approaches.[5] Planar defect-free nanographenes of different sizes, shapes, lengths, widths or edge structures have been reported going from coronene or hexa-*peri*-hexabenzocoronene (HBC) as the basic representative models to extraordinary extended PAHs or large graphene nanoribbons (GNR) giving rise to a fine tuning in the optical and electronic properties displayed.[6]

Embedding pentagons in polycyclic arenes originates bowl-shape positive curvatures as in fullerene fragments[7] or carbon nanotubes end caps.[8] From the first synthesis of corannulene in 1966 many aromatic molecular-bowl hydrocarbons have been presented and studied.[9]

In contrast to the case of pentagons, the introduction of seven- or eight-membered carbocycles into a hexagonal planar network induces a negative curvature with saddle shape.[1d] The interest on carbon structures containing negative curvature has been evidenced for more than twenty years with theoretical[10] and experimental[2a] studies pointing out the potential impact over the geometry and properties of the basic sp^2 planar system. However, it has been recently when those curved distorted carbon nanostructures are receiving increasing attention. It is expected that this kind of curvature might have important impact on the opto(electronic) properties and consequently on their possible applications.[11]

Nanographenes containing heptagons or octagons are still much less common than including pentagons.[12] The controlled introduction of those defects in carbon nanomaterials is only possible if suitable synthetic routes to produce such defects are available. Within this context, bottom-up approaches (benchtop) to carbon-based nanostructures are essential since they provide homogeneous and well-defined materials with novel structures and geometries. On the unequivocal characterization of those carbon-based structures lays the foundation for their future applications.

Herein we highlight relevant recent progress on the synthetic strategies developed for the preparation of well-defined heptagon-embedded polycyclic arenes with special focus on the results reported by our group. Particular attention is given to the synthetic strategy employed to obtain the target heptagon, responsible for the negative curvature in the otherwise planar network, and some insights into the opto(electronical)

[a] Departamento Química Orgánica. Universidad de Granada (UGR). C. U. Fuentenueva, 18071 Granada, Spain. E-mail:araceligc@ugr.es
† Those authors contributed equally to this work.

properties of the carbon nanostructures prepared are also briefly commented. Finally, synthetic strategies towards the preparation of saddle-shape PAHs containing eight-membered carbocycles are also included.

2. Bottom-up Synthesis of Saddle Nanographenes

The synthesis of well-defined nanographenes took off with several synthesis of representative hexabenzocoronene (HBC) reported by Clar, Halleux and Schmidt in the last century.[13] Later on, the seminal works developed by Müllen and co-workers in obtaining HBC through oxidative intramolecular cyclodehydrogenation of hexaphenylbenzene layed the basis for the synthesis of new π-extended PAHs.[14] Synthetic approaches toward adequate oligophenylenes based on Co-catalyzed cyclotrimerization of diphenylacetylene derivatives or on Diels-Alder cycloaddition between tetraphenylcyclopentadienone and diphenylacetylene derivatives have been widely employed giving rise to functionalized oligophenylenes. From them, PAHs can be prepared by a variety of synthetic methodologies achieving high efficiency and novelty.[6b-e,15] Among them, the selective oxidative aromatic coupling of unfunctionalized arenes with a net loss of hydrogens[15b] has become the most popular synthetic route to nanographenes especially leading by the contributions of Müllen's group.[16]

The possibility of designing and controlling the synthesis of nanographenes allows the introduction of designed defects on the aromatic structure in order to cause distortions away from planarity. This alteration in the aromatic structure results in novel shapes and changes in the electronic and optical properties of the obtained nanographenes.

Within the bottom-up approaches based on organic synthesis for the preparation of well-defined distorted saddle-shape nanographenes, three main strategies have been used to create the key heptagonal carbocycle. Firstly, the direct use of a functionalized seven-membered carbocycle as starting material and subsequent creation of the surrounding aromatic backbone in consecutive steps (Scheme 1a). A second approach that has been quite extensively used consists on the generation of the heptagon by means of an intramolecular closing reaction mainly by a final oxidative cyclodehydrogenation although Friedel-Craft reaction has also been used (Scheme 1b). Recently, Miao *et. al.*, have reported an alternative approach in which a ring expansion reaction of cyclohexanone moieties gives rise to the central heptagon in the hexagonal lattice (Scheme 1c). In our approach, we create the seven-membered ring by an adequate intermolecular cyclotrimerization reaction of simple starting materials, namely dialkynes **I** and diarylacetylenes **II** (Scheme 1d). In this case a heptagon-containing polyphenylene is directly created in one single step. Furthermore, the incorporation of functional groups allows the control of the created nanographene and also further expansion of the sp^2 network.

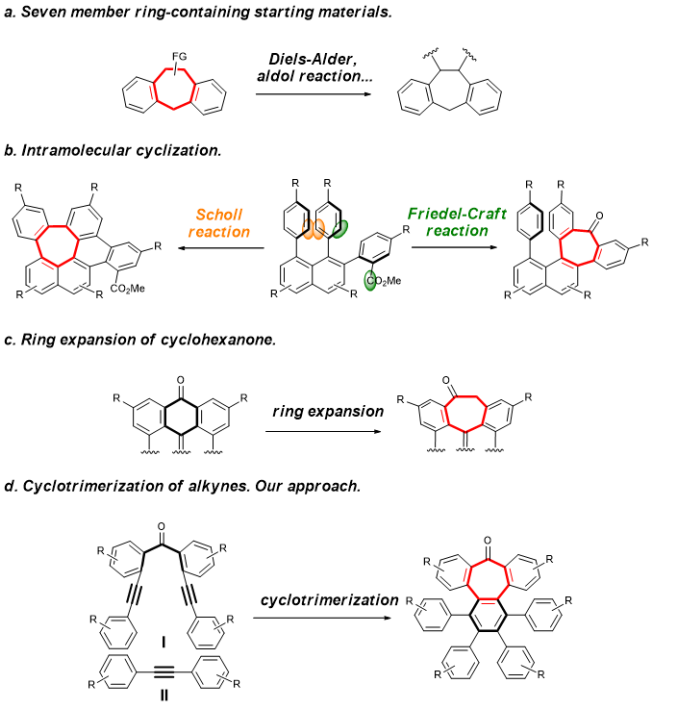

Scheme 1. General approaches for the synthesis of PAHs containing heptagons.

2.1 Synthesis and characterization of PAHs containing heptagons

The archetypal example of a saddle-shaped polycyclic arene is the [7]circulene, whose synthesis was firstly reported by Yamamoto *et. al.*[17] In this approach the key heptagonal ring is created by a photocyclization of flexible biphenylnaphthalene cyclophane **1** (Scheme 2A). The incorporation of adequate functional groups in the starting cyclophane is required for subsequent functionalization and final McMurry reaction leading to [7]circulene **3**. The twisted saddle-shaped structure with C_2 symmetry was confirmed by X-Ray crystallography (Scheme 2B). The Yamamoto group also reported the synthesis of [7.7]circulene following a similar synthetic route.[18] A second approach towards [7]circulene involving a vacuum pyrolysis at 550 °C of bridged-hexahelicene and a final dehydrogenation at 280 °C was also presented.[19]

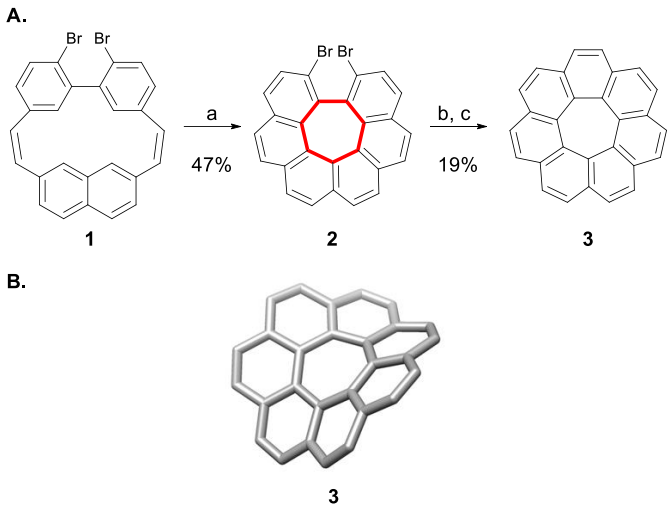

Scheme 2. A. Synthesis of compound **3**. Reagents and conditions: (a) I_2, cyclohexane, hv, 2 h; (b) (i) ^{n}BuLi, THF, –78 °C, 30 min; (ii) DMF, –78 °C, 1 h; (c) $TiCl_3$, $LiAlH_4$, DME, reflux, 4 h. THF = tetrahydrofuran; DMF = dimethylformamide; DME = dimethoxyethane. **B**. X-ray crystal structure of compound **3** (hydrogen atoms are omitted for clarity).

After those groundbreaking examples reported in the late eighties, surprisingly the synthesis of heptagon-containing PAHs remained almost unexplored for more than 20 years until 2012, when Q. Miao and co-workers synthesized a heptagon-embedded PAH with negative curvature and π-isoelectronic to the planar hexa-*peri*-benzocoronene (HBC).[20] They followed the synthetic strategy developed by Müllen to obtain substituted HBC,[6b,21] being the key steps a Diels-Alder cycloaddition to create the basic aromatic backbone and a Scholl-type oxidative cyclodehydrogenation leading to the nanographene structure. In this case, the seven-membered ring is already incorporated in the dienophile precursor **4** used in the Diels-Alder reaction (Scheme 3A). The final cyclodehydrogenation reaction was performed with $FeCl_3$ acting simultaneously as Lewis acid and oxidant. As previously reported by King, they found that the position of alkoxyl groups were determinant in this reaction.[22] These activating substituents should be located in the *ortho* or *para* positions to the reaction sites, otherwise the desired product could not be isolated from the complex mixture obtained.

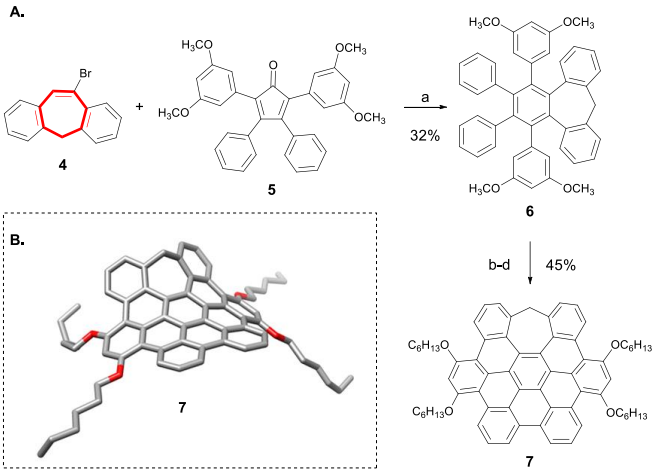

Scheme 3. A. Synthesis of compound **7**. Reagents and conditions: (a) ^{t}BuOK, Et_2O, rt, 24 h; (b) BBr_3, CH_2Cl_2, reflux, 4 h, 89%; (c) $C_6H_{13}Br$, K_2CO_3, DMF, 85 °C, 16 h, 81%; (d) $FeCl_3$, CH_3NO_2, CH_2Cl_2, rt, 3 h, 62%. **B**. X-ray crystal structure of compound **7** (hydrogen atoms are omitted for clarity).

The structure of this new saddle-shaped PAH **7** was resolved by X-ray crystallography showing a great distortion from planarity with negative curvature (Scheme 3B). The intercalated long alkyl chains between the curved aromatic networks prevent π-interactions between molecules, as observed in the molecular packing of **7**. Interestingly, **7** exhibited green fluorescence when irradiated with UV light and similar wavelength absorption to HBC but with much higher extinction coefficient.

Almost simultaneously, Kuck and co-workers reported the synthesis of a PAH containing a seven-membered carbocycle.[23] In this case, a bowl-shaped tribenzotriquinacene (TBTQ) is fused with a pentaphenylphenyl unit (Scheme 4, **8**). Final Scholl reaction using $Cu(OTf)_2/AlCl_3/CS_2$ combination, as Lewis-acidic conditions, led to the expected TBTQ-HBC scaffold and also generated a cycloheptatriene that bridges both units. Thus, the saddle-shaped heptagon connects the bowl-shaped TBTQ with the planar HBC. Remarkable, they found that in this case, the use of $FeCl_3$ only gave the starting materials in the oxidative cyclodehydrogenation.

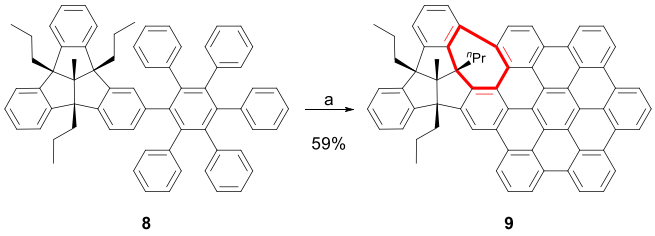

Scheme 4. Synthesis of compound **9**. Reagents and conditions: (a) $AlCl_3$, $Cu(OTf)_2$, CS_2, 45 °C, 30 h.

However, in 2013, Durola *et al*. unexpectedly obtained an unusual twisted PAH **11** incorporating a seven-membered carbocycle that is created by a rearrangement during an

intramolecular Scholl reaction mediated by $FeCl_3$.[24] The structure of **11** was confirmed by X-ray crystallography, revealing that it is highly distorted due to the presence of one [5]helicene and one seven-membered ring as part of a hexa[7]circulene.

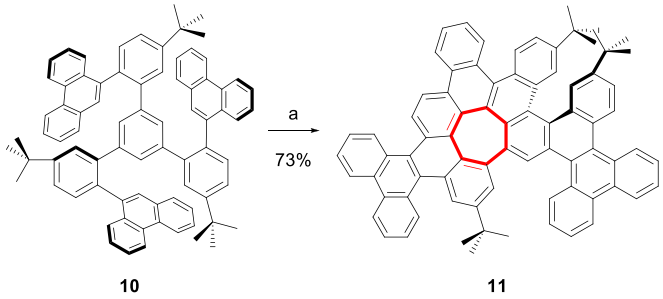

Scheme 5. Synthesis of compound **11**. Reagents and conditions: (a) $FeCl_3$, CH_2Cl_2, CH_3NO_2, rt, 1 h.

Also in 2013, Itami, Scott and co-workers reported one of the seminal examples in the area of distorted saddle-arenes. They presented the synthesis of an extraordinary distorted warped nanographene bearing six seven-membered rings surrounding a corannulene core by means of a remarkable straightforward synthetic route.[25] The synthesis consisted in a palladium catalyzed C–H activation of commercially available corannulene, followed by a cyclodehydrogenation reaction which 'ran to the end' giving the warped $C_{80}H_{30}$ **15** and $C_{120}H_{110}$ **16**. This two-steps procedure manages to multiply by four the number of carbon atoms in the conjugated backbone and to form 10 new rings, including five strained heptagons in a single cyclization step. Once again, the formation of the strained heptagonal rings occurs during a cyclodehydrogenation reaction, either by $FeCl_3$ or by the combination of 2,3-dichloro-5,6-dicyano-*p*-benzoquinone (DDQ) and trifluoromethanesulfonic acid (triflic acid, TfOH). As confirmed by the X-ray crystal structure, compound **15** exists as a pair of enantiomers, (*P,M,P,M,P*) and (*M,P,M,P,M*), according to the *P* or *M* chirality of each of the hexa[7]circulene moieties conforming their structures, although ^{1}HNMR showed rapid racemization in solution. Moreover, the high level of distortion in compound **15** confers great solubility and perturbs its electronic and optical properties. Compared with the similar-size planar nanographene obtained by Müllen and co-workers in 2000,[5a] the calculated band valence gap (HOMO-LUMO energy difference) of **15** is larger than that for the planar counterpart due to a lowering of the HOMO, while the LUMO remains similar for both compounds. Also the UV-vis spectrum of **15** was blue-shifted respect to that of the planar PAH and, unlike this, **15** presented fluorescence. Thanks to its good solubility, cyclic voltammetry measurements of **15** could be performed. It showed three reversible reduction potentials associated with the presence of a five-membered ring in the structure which is known because of its ability to impart good electron-accepting character, as in the case of corannulene or C_{60} fullerene. Moreover, compound **15** showed two reversible oxidation potentials, which are not common in this type of structure and were attributed to the presence of the seven-membered rings included in its warped framework. These results highlight the effects of distorting the π-surface regarding to the electronic and optical properties of PAHs and prompt to the development of new negatively-curved nanographenes.

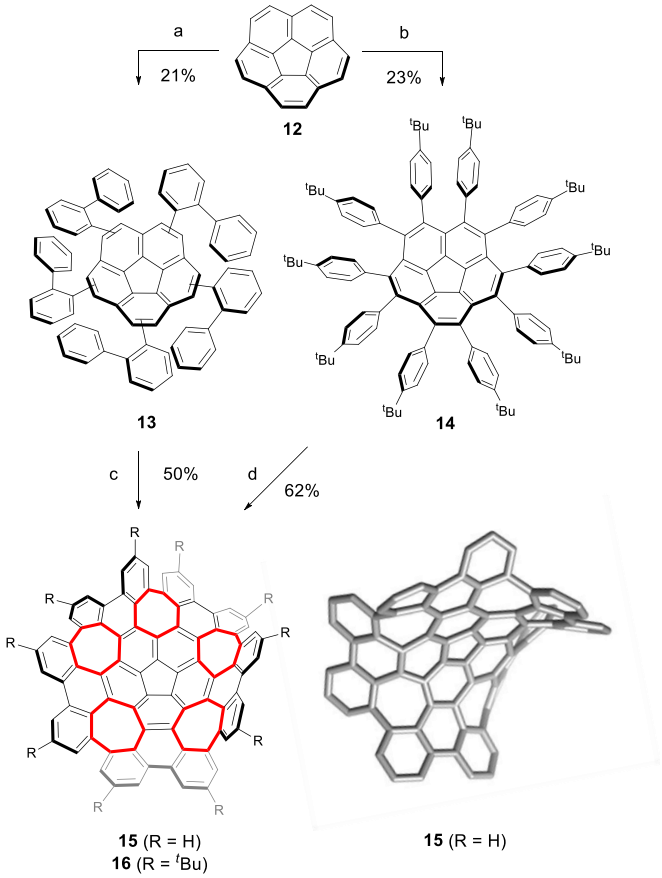

Scheme 6. Synthesis of compounds **15** and **16** and X-ray crystal structure of **15** (hydrogen atoms are omitted for clarity). Reagents and conditions: (a) tris-(*o*-biphenyl)boroxin, $Pd(OAc)_2$, *o*-chloranil, DCE, 80 °C, 16 h; (b) tris-(*p*-(*t*-butyl)phenyl)boroxin, $Pd(OAc)_2$, *o*-chloranil, DCE, 80 °C, repeat for 3-4 cycles; (c) DDQ, CF_3SO_3H, CH_2Cl_2 0 °C, 30 min; (d) $FeCl_3$, CH_2Cl_2, CH_3NO_2, rt, 1 h. DCE = dichloroethane; DDQ = 2,3-dichloro-5,6-dicyanobenzoquinone.

Following this trend, in 2015, (Scheme 7) Miao and co-workers reported the synthesis of two new types of soluble saddle-shaped PAHs bearing two heptagon-embedded rings and they investigated their semiconductor properties in solution-processed thin film transistors.[26] The first seven-membered ring of precursors **22a,b** was directly introduced from the starting material (compound **17**, Scheme 7) in the first step of the HBC derivative synthesis. The aromatic backbone was then created by a Diels-Alder reaction and subsequently, the second seven-membered ring was formed through an intramolecular Friedel-Crafts acylation mediated by methanesulfonic acid after oxidative cyclodehydrogenation with DDQ and triflic acid. The two carbonyl groups in these odd-membered rings served as point to extend the π-surface in both directions. Thus, PAHs **23a,b** were obtained by means of a nucleophilic addition of

fluorenone anions to the carbonyl groups of diketones **22a,b** followed by dehydration under acidic conditions and subsequent oxidative cyclodehydrogenation with DDQ and triflic acid. PAHs **24a,b** were obtained by reacting diketones **22a,b** with CBr_4 in the Corey-Fuchs reaction followed by a Suzuki coupling with phenylboronic acid. Again final oxidative cyclodehydrogenation with DDQ and triflic acid gave the desired distorted compounds **24a,b**. The saddle shapes of **23b** and **24b** were proved by X-ray crystallography. Regarding to their optical properties, extended PAHs **23a,b** and **24a,b** appeared as orange solutions with very weak or almost any fluorescence. This lack of emission was associated with the high flexibility which in solution consumes the energy of the excited state. Both **23a,b** and **24a,b** presented enhanced fluorescence in the solid state attributed to aggregation induced emission (AIE).[27] Preliminary studies of their semiconducting properties showed that polycrystalline films of **23b** and **22b** behaved as p-type semiconductors with field effect mobilities of 1.3×10^{-5} and 6×10^{-4} cm^2 V^{-1} s^{-1}, respectively. In the case of **24b** no field effect mobility was detected. Its insulating behavior was related to the amorphous film obtained when depositing in SiO_2 wafer to create the transistor.

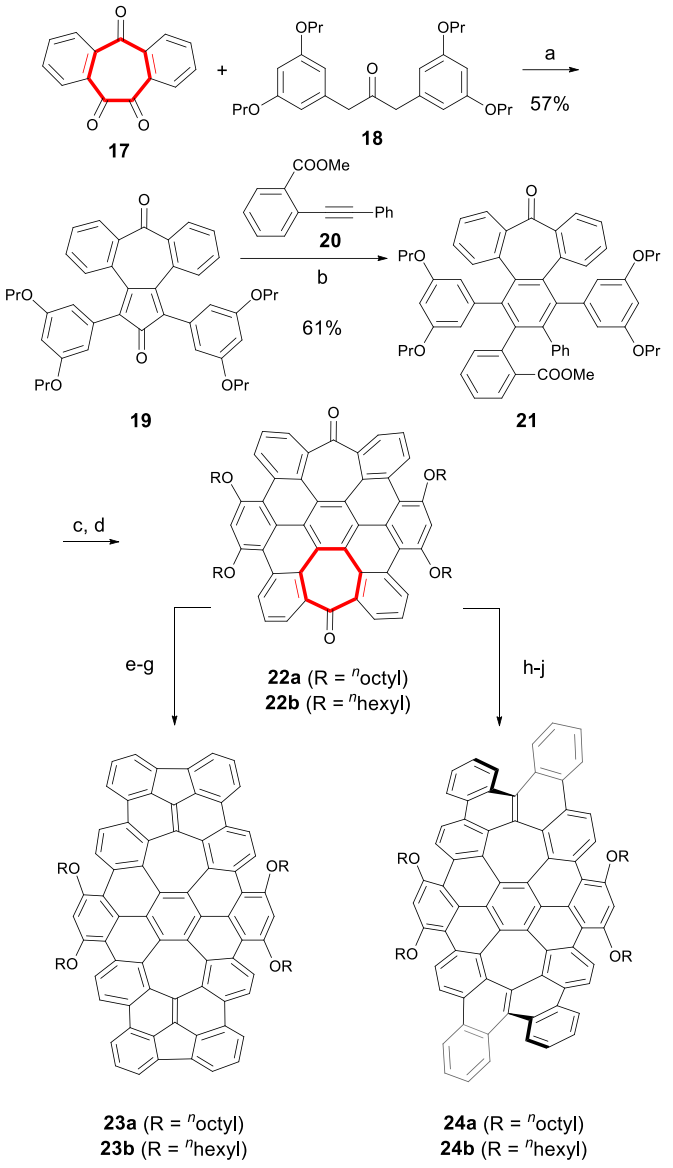

Scheme 7. Synthesis of compounds **23a**,**b** and **24a**,**b**. Reagents and conditions: (a) KOH/MeOH, THF, rt, 4.5 h; (b) diphenyl ether, reflux, 16 h; (c) (i) DDQ, CF_3SO_3H, CH_2Cl_2, rt, 1 h; (ii) CH_3SO_3H, 80 °C, 4 h, 45%; (d) (i) BBr_3, CH_2Cl_2, reflux, 4 h; (ii) K_2CO_3, RBr, DMF, 80 °C, 16 h, 42% (R = ^{n}octyl), 43% (R = ^{n}hexyl); (e) ^{n}BuLi, fluorene, THF, rt to reflux, 6h, 93% (R = ^{n}octyl), 91% (R = ^{n}hexyl); (f) TsOH, Ac_2O, toluene, reflux, 48 h, 52% (R = ^{n}octyl), 70% (R = ^{n}hexyl); (g) DDQ, CF_3SO_3H, CH_2Cl_2, rt, 3h, 40% (R = ^{n}octyl), 45% (R = ^{n}hexyl); (h) PPh_3, CBr_4, toluene, reflux, 16 h, 93% (R = ^{n}octyl), 84% (R = ^{n}hexyl); (i) phenylboronic acid, $Pd(PPh_3)_4$, K_2CO_3, toluene, H_2O, EtOH, reflux, 36 h, 70% (R = ^{n}octyl), 37% (R = ^{n}hexyl); (j) DDQ CF_3SO_3H, CH_2Cl_2, rt, 1h, 81% (R = ^{n}octyl), 63% (R = ^{n}hexyl). TsOH = *p*-toluenesulfonic acid.

A few years later Kuck and co-workers presented the synthesis of a new TBTQ-based non-planar polyaromatic compound **26** bearing three cycloheptatriene rings formed through a three-fold Scholl-type cyclization reaction (Scheme 8).[28] They proposed the resulting wizard hat-shaped molecule as a promising intermediate for the development of larger π-extended nonplanar nanographenes. TBTQ derivative **25** was treated with a DDQ/TfOH system after unsuccessful results with other oxidative systems ($FeCl_3/MeNO_2$, $AlCl_3/Cu(OTf)_2$, $MoCl_5$) giving three-fold cyclization to **26**.[28a] Compound **26** is soluble in

most organic solvents, resulting in an orange solution with weak purple fluorescence when irradiated with UV light.

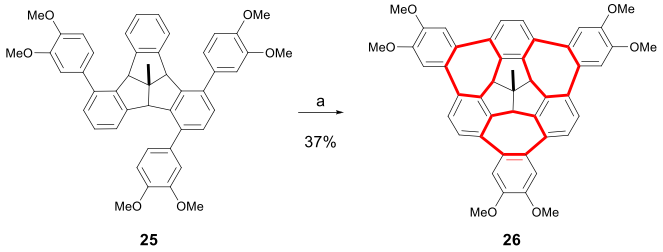

25 26

Scheme 8. Synthesis of compound **26**. Reagents and conditions: (a) DDQ, CF_3SO_3H, CH_2Cl_2, 0 °C, 24 h.

More recently, in 2017, Miao and co-workers reported the synthesis of a tetrabenzo[7]circulene **27**, a new member of the saddle-shaped PAH with high flexibility and also p-type semiconductor properties.[29] In this case, the centered heptagon is isolated in the first step by an intramolecular Friedel-Craft acylation in $NaCl/AlCl_3$ at 150 °C leading to 5,12-pleiadenedione in a low 15% yield. Subsequently, the surrounding aromatic backbone is built stepwise. Tetrabenzo[7]circulene **27** has four extra benzene rings compared with [7]circulene and it bears two [4]helicenes giving rise to two enantiomers denoted as (*P*,*M*,*P*) and (*M*,*P*,*M*) according to the chirality of one of the [4]helicenes, the seven-membered ring, and the other [4]helicene, respectively. Both of them were observed in the crystal structure of **27** (Fig. 1). Green fluorescence is observed when the yellow solution of compound **27** in CH_2Cl_2 is irradiated with UV light. Its longest wavelength absorption maxima appears about 80 nm red-shifted respect to that of [7]circulene. Although with a low field effect mobility (5×10^{-4} cm^2 V^{-1} s^{-1}), compound **27** functioned as a p-type semiconductor in ambient air. A solution of **27** and C_{60} in *o*-dichlorobenzene led to cocrystallization of **27** and C_{60} in a ratio of 1:1 as observed by X-ray crystallization. Considering the p-type semiconductor properties of **27** and the n-type semiconductor properties of fullerenes, the cocrystals of both compounds were proposed as interesting for applications in solar cells.

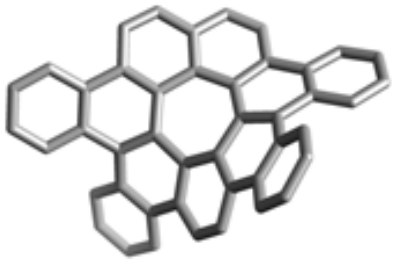

27

Fig. 1. X-ray crystal structure of compound (*P*,*M*,*P*)-**27** (hydrogen atoms are omitted for clarity).

Continuing with the pursuit of highly distorted frameworks,[30] Itami and co-workers prepared a laterally π-extended dithia[6]heliceneas the foundation towards the preparation of helical hybrid nanoarchitectures.[31] In this case, again unexpectedly, a seven-membered carbocycle is obtained during an oxidative cyclodehydrogenation reaction, this time in the presence of excess of $MoCl_5$ using oxygenated-saturated dichloromethane as solvent (Scheme 9). In situ chlorination is also observed and then Pd-mediated dechlorination yielded compound **30.** In this case, the aromatic surface extends around the helicene structure and, despite the lateral π-extension of helicenes has become frequent in recent years,[32] this was the first example of a helix fully fused with polyaromatic moieties. The structure of **30** was confirmed by ^1H and ^{13}C NMR spectra and mass spectrometry. Also X-ray crystallography corroborated the assumed distortion of the π-surface caused by three structural components: a helical dithia[6]helicene motif, a saddle-shaped dithiahexa[7]circulene motif, and relatively planar bilateral motifs. The high isomerization barrier (49 Kcal mol^{-1}) allowed the chiral resolution of both enantiomers and chiroptical measurements. The UV-vis absorption spectrum of **30** exhibits an intense absorption around 400 nm and a structured absorption band between 450-525 nm with clear vibronic features. The fluorescence spectrum gave maxima at 514 and 548 nm for **30** reaching quantum yield of 0.23.

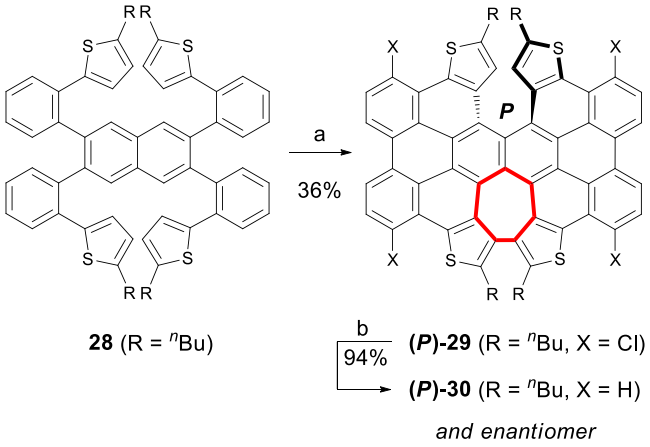

28 (R = ^{n}Bu)

Scheme 9. Synthesis of compound **30**. Reagents and conditions: (a) $MoCl_5$, CH_2Cl_2, rt, O_2, rt, 27 h; (b) Pd/C, HCOOH, Et_3N, pyridine, 130 °C, 72 h.

The curvature induced by the use of seven-membered rings to bridge together two planar π-extended units was also demonstrated in the case of Ni and Zn-porphyrins by Osuka, Kim and co-workers.[33] While conventional porphyrin ribbons took on rigid and planar structures, these porphyrin arch-tapes shown remarkably contorted structures, high conformational flexibility and remarkably good solubility due to the presence of the seven-membered ring(s). In this case, the heptagonal bridge is again obtained by Scholl reaction promoted by the combination of DDQ/$Sc(OTf)_3$.

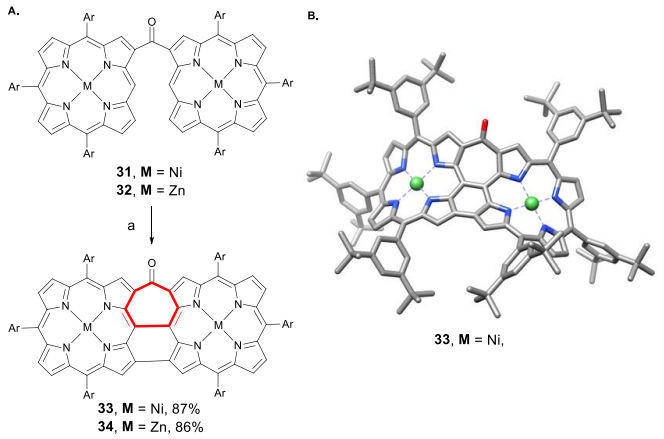

Scheme 10. A. Synthesis of metalloporphyrins **33** and **34**. Reagents and conditions: (a) DDQ, $Sc(OTf)_3$, toluene, 60 °C, 2 h. Ar = 3,5-di-*tert*-butylphenyl. **B.** X-ray crystal structure of compound **33** (hydrogen atoms are omitted for clarity).

Despite the versatility offered by Scholl oxidation in the intramolecular creation of large PAHs, its full control remains still an unsolved challenge.[15b,22] It is known that rearrangements readily occur in Scholl reactions and interfere with the construction of certain molecular architectures.[34] This is the case of one study presented by Tobe and co-workers, where they reported the unexpected results obtained under Scholl reaction conditions.[35] In this case, by X-ray crystallographic analysis they confirmed that treatment of a twisted PAH containing a cyclooctatraene with either $FeCl_3/CH_3NO_2$ or $DDQ/Sc(OTf)_3$ originated a skeletal rearrangement giving polycyclic aromatic compound **36** containing a seven-membered ring.

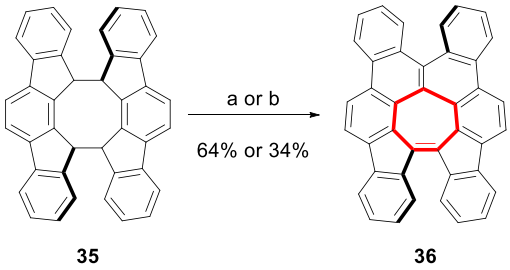

Scheme 11. Synthesis of compound **36**. Reagents and conditions: (a) $FeCl_3$, CH_3NO_2, CH_2Cl_2, rt, 1 h; (b) DDQ, $Sc(OTf)_3$, toluene, 80 °C, 13 h.

Despite the impressive examples reported so far in the area of saddle-arenes, efficient and versatile methods for the synthesis of heptagon-containing PAHs are still required. In previous approaches, the key seven-membered carbocycle is either directly introduced from heptagonal precursors or created through final intramolecular cyclodehydrogenation or Friedel-Craft reactions. These bottom-up syntheses provide well-defined π-extended distorted PAHs and represent a takeoff within this field, although some limitations might arise. Thus, the direct use of heptagonal precursors requires subsequent stepwise expansion, while oxidative cyclodehydrogenation reaction is difficult to predict and control.

Recently our group reported an alternative straightforward strategy to obtain saddle-shaped polycyclic arenes (Scheme 1d).[36] In this case, the key seven-membered carbocycle is generated at once, simultaneously with the polyphenylene structure by a Co(0)-mediated intermolecular cyclotrimerization reaction. Subsequent cyclodehydrogenation reaction affords distorted heptagon-containing nanographenes adequately functionalized for further expansion of the aromatic backbone (Scheme 12).

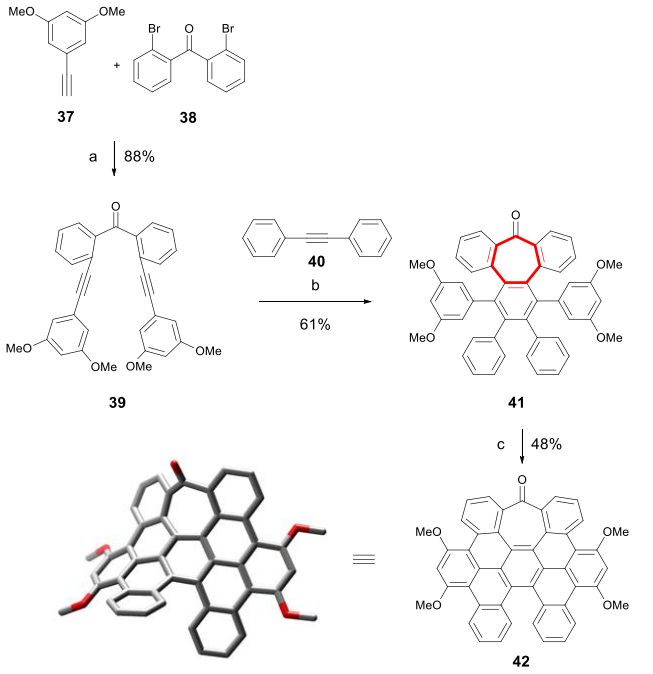

Scheme 12. Synthesis and X-ray structure of compound **42** (hydrogen atoms are omitted for clarity). Reagents and conditions: (a) $PdCl_2(CH_3CN)_2$, CuI, $P(^tBu)_3HBF_4$, $iPrNH_2$, THF, rt, 2 h; (b) $Co_2(CO)_8$, dioxane, 100 °C, 16 h; (c) DDQ, CH_3SO_3H, CH_2Cl_2, rt, 30 min.

Starting dialkynes and diphenylacetylene derivatives (e.g. **39** and **40**) can be easily prepared from simple precursors via Sonogashira-Hagihara coupling reactions. The versatility of our method relays on the variety of precursors that can be used, bearing functional groups in different positions that are directly incorporated in the final distorted PAH. Thus, we obtained in one single step three key features of the final distorted PAHs: i) the heptagonal ring, ii) the polyphenylene structure and iii) the functional groups in selected positions. Those functional groups such as methoxy groups, played a dual role; firstly as activating groups directing the final cyclodehydrogenation reaction by DDQ/acid combination and secondly as reactive point to further expand the aromatic network. In this case, OMe groups were also used as electrophiles in Ni-catalyzed Kumada-Tamao-Corriu reaction[37] using (*p*-*tert*-butylphenyl)magnesium bromide in the presence of $Ni(cod)_2$ and PCy_3 in refluxing toluene (Scheme 13). Thus, four new aromatic rings are introduced in one step, and final oxidative dehydrogenation led to new highly distorted PAHs. Unexpectedly, an adjacent combination of a

five- and seven-membered carbocycles is formed from **43b**, as revealed by the X-ray crystallography of **45**. The polycyclic backbone of **45** has a curved shape caused by the pentagon-heptagon unit and the chiral twisted conformation caused by the [5]helicene moiety. Its distortion from planarity avoids strong π-π interactions between molecules and therefore enhances solubility in common organic solvents . Remarkably, both compounds **44** and **45** resulted luminiscent when irradiated with UV light, with similar quantum efficiency (ϕ) of 7.2 and 7.5 %, respectively. Moreover, these distorted nanographenes showed an exceptional long fluorescence lifetimes of 14.5 and 12.9 ns which are significantly longer than that of related fluorescence dyes, such as perylene bisimides.[38] Moreover, the HOMO-LUMO energy gap for **44** and **45** based on the first half-wave oxidation and reduction potentials, resulted in 2.66 eV and 2.27 eV, respectively, which are in the range of previously described extended aromatic systems.[39]

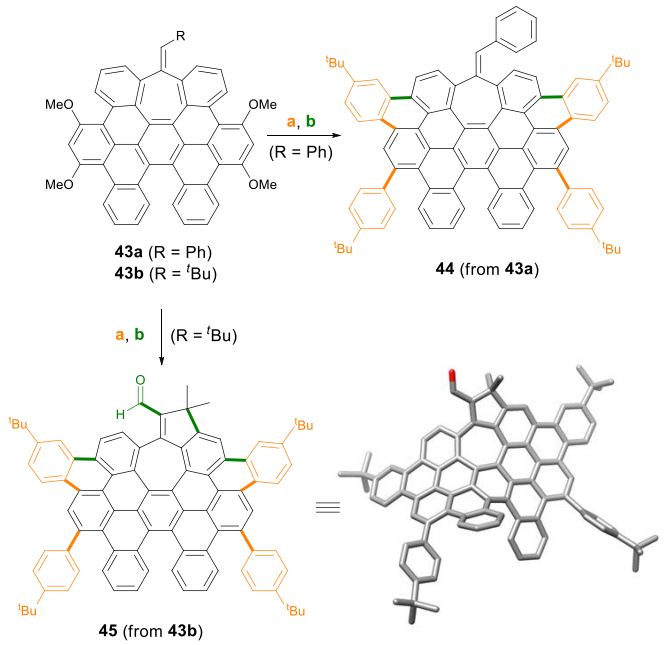

Scheme 13. Synthesis of compounds **44** and **45** and X-ray crystal structure of **45** (hydrogen atoms are omitted for clarity). Reagents and conditions: (a) $Ni(cod)_2$, PCy_3, *p*-^{t}BuPhMgBr, toluene, 100 °C, 16 h, 79% (for R = Ph), 59% (for R = ^{t}Bu); (b) DDQ, CH_3SO_3H, CH_2Cl_2, 47% (for R = Ph), 44% (for R = ^{t}Bu). cod = 1,5-cyclooctadiene; Cy = cyclohexyl.

As commented above, this synthetic strategy gives rise to heptagon-containing polyphenylenes (Scheme 12, **41**) in a straightforward manner. Those bulky propeller-like groups have also proved as efficient stoppers to sterically protect reactive moieties avoiding intermolecular interactions while enhancing solubility.[40] Thus, the ketone moiety in the tropone unit allows the incorporation of those saddle-shaped polyphenylenes as endgroups on [3]cumulenes resulted in the luminescence activation of the latter upon aggregation (Scheme 14, **46**). Sterical protection avoids the aggregation of the planar conjugated [3]cumulenes which would quench their emission. While solvation allows the rotation of their phenyl rings leading to non-emissive solutions, upon aggregation, the restriction of their intramolecular motions resulted in high fluorescence emission yields, in an aggregated induced emission process (AIE), reaching a remarkable quantum yield value of ca. 64% in 70 vol % water content in THF. Besides, the two-photon absorption based upconversion (TPA-UC) of the [3]cumulene **46** aggregates was also shown. Therefore, the use of these heptagon-containing polyphenylenes as protective groups opens up the possibility of using [n]cumulenes as active luminogens upon aggregation. Other heptagon-containing AIE active compounds have also been reported based on the restriction of intramolecular vibration (RIV).[27,41]

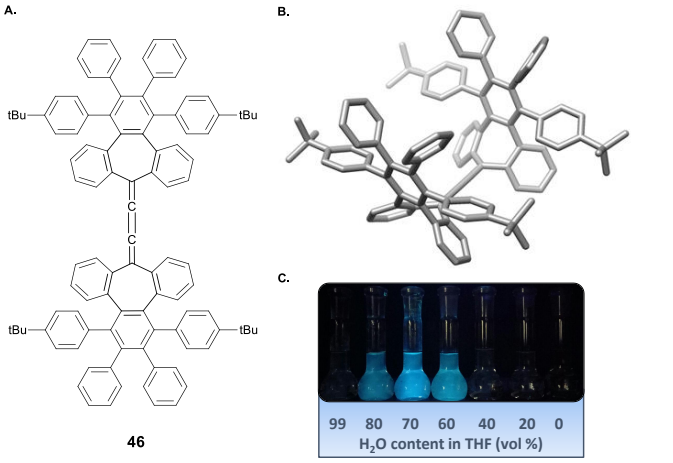

Scheme 14. A. Structure of [3]cumulene **46**. **B**. X-ray crystal structure of **46** (hydrogen atoms are omitted for clarity). **C**. Photograph of **46** in THF/water mixtures taken under illumination of a UV lamp.

The easy introduction of functional groups in selected positions of the distorted nanographenes network facilitates a direct and controlled creation of molecular diversity. In this sense, the precise introduction of defects in nanographenes can implement interesting new combinations of optical properties. Following this idea, we have recently reported the synthesis of an enantiopure distorted ribbon-shaped nanographene that combines i) an electron rich π-extended ribbon aromatic network, ii) a non-racemizable [5]helicene moiety and iii) an aromatic saddle-shaped ketone unit as a tropone moiety.[42] Starting from saddle-nanographene **47** incorporating bulky *t*-Bu groups and an electrophile such as iodine in selected positions, the synthesis of ribbon-shaped nanographene **51** was accomplished in only three steps (Scheme 15) by Sonogashira coupling with *p-tert*-butylphenylacetylene, subsequent Diels-Alder reaction with cyclopentadienone **49** and final oxidative cyclodehydrogenation reaction with DDQ/TfOH mixture.

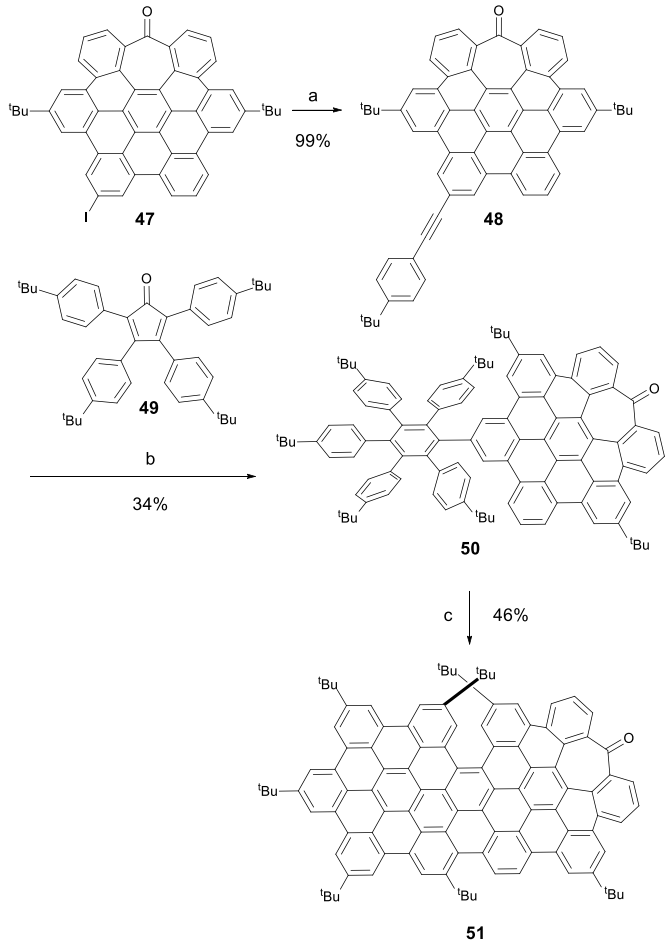

Scheme 15. Synthesis of compound **51**. Reagents and conditions: (a) 4-*tert*-butylphenylacetylene, $PdCl_2(PPh_3)_2$, CuI Et_3N, THF, rt, 16 h; (b) Ph_2O, reflux, 8 h; (c) DDQ, CF_3SO_3H, CH_2Cl_2, 0 °C, 10 min.

Bearing these structural features, distorted PAH **51** exhibited unprecedented combination of optical properties, namely TPA-UC with circularly polarized luminescence (CPL). Chiral molecules able to produce circular polarized luminescence responses are of increasing interest due to their promising applications in optical devices and biosensors.[43] Organic molecules with π-conjugated structures and chiral moieties such helicenes have been extensively reported as CPL-active compounds.[44]

In this case, the kinetically stable [5]helicene in **51** allowed chiral resolution of both enantiomers.[45] Although helical PAHs have been extensively reported,[30,32e,46] remarkably, compound *M/P*-**51** is the first example reported of the CPL emission for an enantiopure nanographene. The structure of compound **51** was confirmed by X-ray crystallography (Fig. 2) revealing the saddle-shape curvature in the aromatic backbone caused by the presence of the heptagon, reaching deviation from planarity with angles up to 24° between the mean plane of the aromatic ring next to the heptagon and the mean plane of the hexagonal planar region. The warped conformation caused by the difunctionalized [5]helicene moiety originates one of the highest torsion angle (θ) reported (ca. 30°) for a [5]helicene.[45] This torsion resulted in a very high solubility (up to 16 mg/mL in CH_2Cl_2) considering the size of the π-surface constituted by 25 aromatic rings.

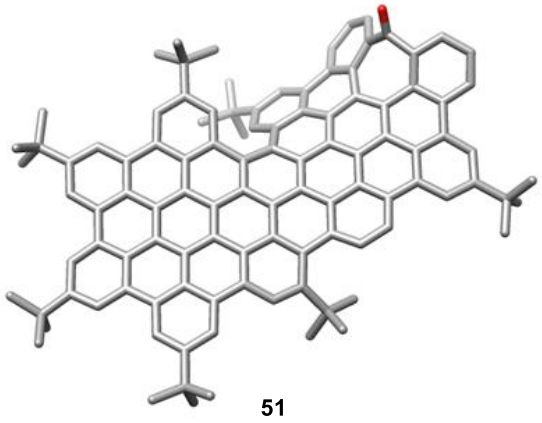

Fig. 2. X-ray crystal structure of compound **51** (hydrogen atoms are omitted for clarity).

The optical properties of **51** were evaluated by one- and two-photon absorption and emission as well as chiroptical properties by means of circular dichroism (CD) and CPL. To sum up, doubly distorted PAH **51** showed absorption and emission maxima at 444 and 560 nm, respectively, reaching fluorescence quantum yield (ϕ) of 13% and very long emission lifetime of 21.5 ns. Moreover, the CPL spectrum of enantiopure *M*/*P*-**51** showed an emission maxima at 560 nm upon irradiation with UV light (λ_{exc} = 372 nm) matching the same energy transition observed for the upconverted emission upon two-photon absorption (λ_{exc} = 770 nm), which represents an unprecedented process of TPA-based upconverted CPL. The resulted g_{lum} for **51** was 2.3×10^{-4}, it represents the first reported circularly polarized emission for an enantiopure nanographene. Supported by DFT-calculations, it was concluded that the presence of the heptagon unit and the possibility of having a charge transfer between the chiral moiety and the heptagon are favorable for both the chiroptical and the two-photon absorption.

Very recently (2018), Miao and co-workers have presented a new negatively curved nanographene, which contains an unprecedented pattern of two heptagons, centered on a tetrabenzodipleiadiene moiety (Scheme 16).[47] In this case, the heptagonal carbocycle is obtained by a new and alternative strategy through a ring expansion reaction of cyclohexanone moieties in a tetra(*t*-butyl)bisanthenequinone. $TMSCHN_2$ was used to accomplish the ring expansion of **52** resulting in diketone **53**. This intermediate was treated with LDA followed by quenching with triflic anhydride giving ditriflate **54**. Similarly to their previous work,[20] a strained alkyne was generated *in situ* by elimination reaction of **54** with *t*-BuOK reacting, as a dienophile, in the Diels-Alder cycloaddition with cyclopentadienone **49** to afford **55**. Final Scholl-type cyclization either with $FeCl_3$ or with DDQ and triflic acid resulted in **56** as orange solid in very good yields (85% and 81%, respectively).

The saddle-shape of **56** with a greatly curved naphthalene unit at the center was confirmed by X-ray crystallography. Remarkably, DFT calculations probed that *t*-butyl groups attached to the central tetrabenzodipleiadiene moiety of nanographene $C_{86}H_{32}$ can stabilize the saddle conformation and make this nanographene less flexible. Compound **56** showed good solubility in common organic solvents, forming an orange solution in hexane, which exhibited weak yellow luminescence upon irradiation with UV light.

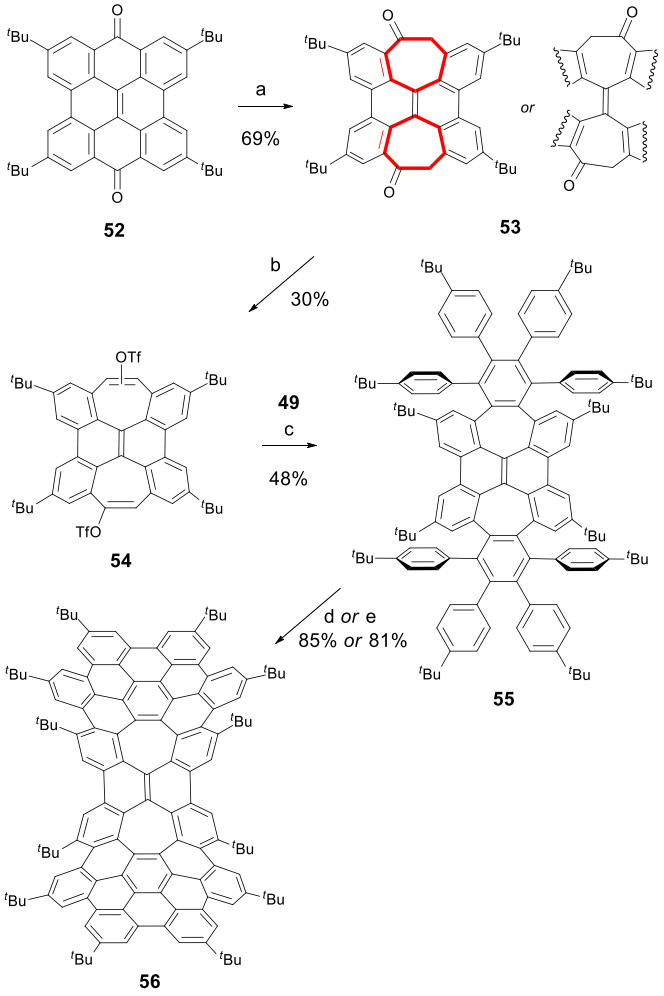

Scheme 16. Synthesis of compound **56**. Reagents and conditions: (a) $TMSCHN_2$, $BF_3.OEt_2$, CH_2Cl_2, 0 °C, 2.5 h; (b) i) LDA, THF, –78 °C, 2 h; ii) Tf_2O, –78 °C to rt, 16 h; (c) ^{t}BuOK, Et_2O, rt, 16 h; (d) $FeCl_3$, CH_3NO_2, CH_2Cl_2, rt, 1 h; (e) DDQ, CF_3SO_3H, rt, 1 h. TMS = trimethylsilyl; LDA = lithium diisopropylamide; Tf_2O = trifluoromethanesulfonic anhydride.

2.2 Synthesis and characterization of PAHs containing octagons

A step further in the introduction of medium size carbocycles as defects in extended polyaromatic systems from a bottom-up synthetic approach consisted in the introduction of [8]circulene moieties which also induce a deep curvature in the aromatic lattice.[48]

The first attempted synthesis of the saddle-shaped molecule [8]circulene was reported in 1976 by Wennerström *et al.*, but the photoreaction used in the final step of their synthetic strategy did not afford the [8]circulene, presumably because of its highly strained structure and instability.[49] Recently, remarkable progress has been done by several groups in the synthesis and structural characterization of a number of [8]circulene derivatives. In 2013, Wu and co-workers presented the first study of *peri*-substituted [8]circulene derivatives elucidating their synthesis, structural analysis and properties.[50] Their synthetic strategy was based on the previous construction of the central eight-membered ring, and then the generation of the peripheral benzenoids *via* a palladium-catalyzed annulation. The structure of [8]circulene **57** was unambiguously characterized by NMR spectroscopy and X-ray crystallography, showing its highly distorted saddle-shaped structure (Fig. 3).

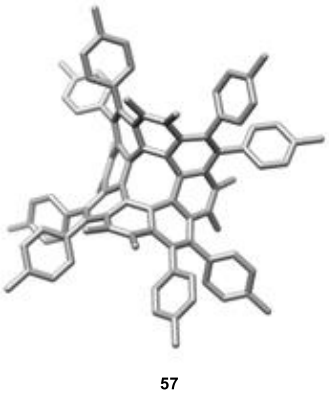

Fig. 3. X-ray crystal structure of compound **57** (hydrogen atoms are omitted for clarity).

Subsequently, Suzuki and Sakamoto presented an elegant and straightforward synthesis of tetrabenzo[8]circulenes **60** and **61** (Scheme 17).[51] In this study the key eight-membered carbocycle was formed in the final step of the synthetic sequence by Scholl reaction of the cyclic octaphenylene precursor **58** and **59** mediated either by $Cu(OTf)_2$, $AlCl_3$ or by $FeCl_3$. The great deviation from planarity and deep saddle-shape structure of tetrabenzo[8]circulene was confirmed by X-ray crystallography.

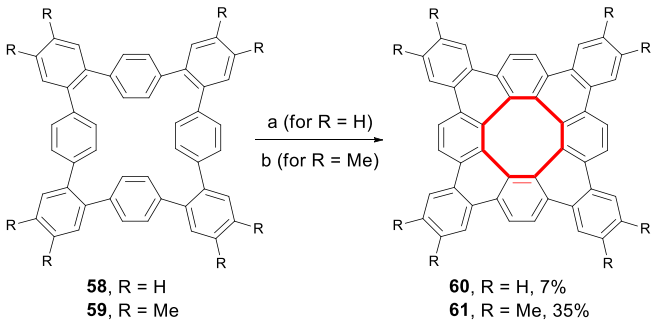

Scheme 17. Synthesis of compounds **60** and **61**. Reagents and conditions: (a) $Cu(OTf)_2$, $AlCl_3$, CS_2, 30 °C, 15 h; (b) $FeCl_3$, CH_2Cl_2, –20 °C, 4 h.

Whalley and co-workers have also described an alternative strategy for the preparation of tetrabenzo[8]circulene **65a-g** (Scheme 18).[52,53] Their synthetic route was based in the previous initial assembly of the eight-membered ring by a Diels-Alder cycloaddition followed either by final palladium-catalyzed arylation or by oxidative cyclodehydrogenation reactions to create the surrounding benzene rings. The latter method presented higher yields and widened the substrate scope, providing access to substrates containing both electron-rich and electron-poor functional groups. Because of its full benzenoid structure, tetrabenzo[8]circulene **65a-g** exhibited a high stability, in contrast to the parent [8]circulene.

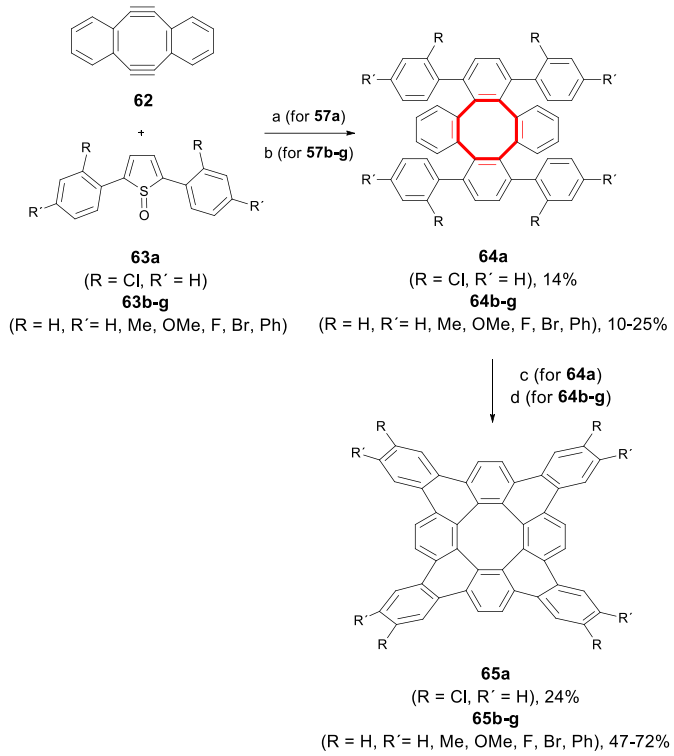

Scheme 18. Synthesis of compound **65a-g**. Reagent and conditions: (a) toluene, 100 °C, 16 h; (b) toluene, 80 °C, 48 h; (c) $Pd(PCy_3)_2Cl_2$, DBU, DMA, mwave, 180 °C, 75 min; (d) DDQ, CF_3SO_3H, CH_2Cl_2, rt, 16 h. DBU = 1,8-diazabicyclo[5.4.0]undec-7-ene; DMA = *N*,*N*-dimethylacetamide.

In 2016, Tobe and co-workers reported the synthesis of twisted polycyclic aromatic hydrocarbon with a cyclooctatetraene (COT) core fused by two indenofluorene units (Scheme 19).[54] The eight-membered ring was obtained after the [4+4] cycloaddition reaction of initial indenofluorene derivative **66**.

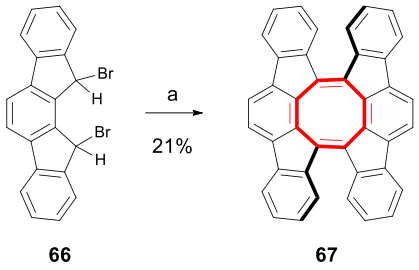

Scheme 19. Synthesis of compound **67**. Reagent and conditions: (a) ^{t}BuOK, THF, 0 °C, 20 min.

Remarkably, in 2017, Miao's group reported the synthesis of a new negatively curved nanographene constituted by 96 sp^2 carbon atoms and presenting the shape of a short twisted ribbon.[55] The novelty of this sort of twistacene is that its curvature arises from an embedded [8]circulene moiety. The synthetic strategy is based on the creation of macrocyclic oligophenylene **68** and final formation of the eight-membered ring by oxidative cyclodehydrogenation reaction mediated by DDQ/TfOH leading to **69**. The crystal structure of **69** led to its unambiguous structure determination, and a pair of enantiomers were found in the crystal having a twisted ribbon-like π-backbone.

Accordingly to the calculated barriers of interconversion, compound **69** resulted more flexible than both [8]circulene and tetrabenzo[8]circulene, as a saddle intermediate conformer facilitates a rapid racemization. Those conformational changes resulted in a non-radiative deactivation of the excited state, and therefore solutions of **69** resulted non fluorescent. Interestingly, luminescence is observed upon aggregation as the restriction of the intramolecular motions activates the radiative emission pathway by an aggregated-induced emission process.[27,56]

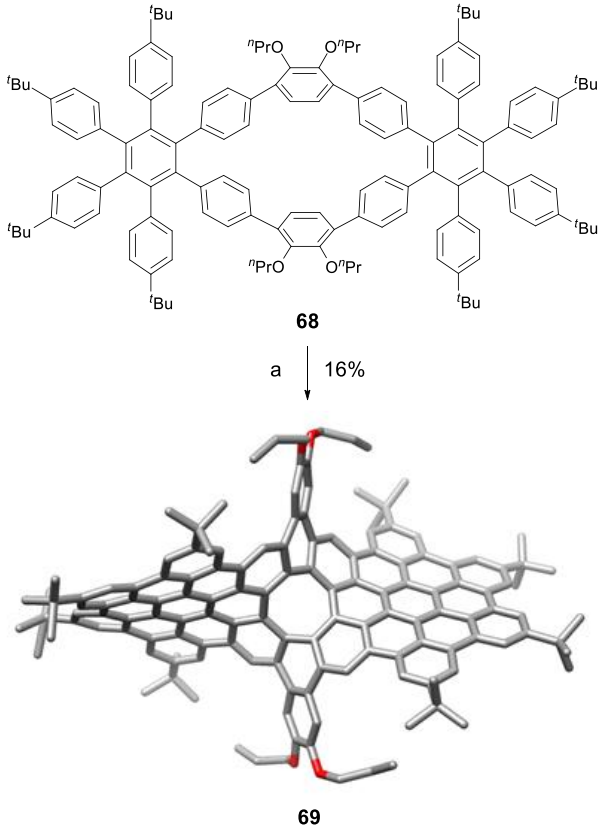

Scheme 20. Synthesis and X-ray crystal structure of **69** (hydrogen atoms are omitted for clarity).

3. Conclusions and perspectives

In this feature article we have collected recent progress on the bottom-up synthesis of well-defined heptagon- and octagon-embedded polycyclic arenes. As shown, the introduction of those medium-size carbocycles in a planar hexagonal network originates highly distorted carbon-based nanostructures with negative curvatures and enhanced flexibility and solubility.

Despite the seminal works reported more than twenty years ago by Yamamoto *et al.* and the great advances also reported on the organic synthesis of purely hexagonal PAHs by Müllen *et al.*, Scott *et al.* and others, the field of saddle-aromatics is still on its early stages, with few relevant examples, mainly reported on recent years. It is expected that the presented synthetic approaches together with other that are yet to come might inspire an important growth of the field.

Furthermore, together with seven- and eight-membered rings, the inclusion of larger carbocycles, the creation of cavities,[57] the inclusion of heteroatoms,[58] or the combinations of defects into sp^2 hexagonal networks of different sizes or shapes, might also be addressed giving rise to newly warped and twisted aromatics.

Within the field of distorted aromatics, the study of helically chiral π-extended sp^2 aromatic networks is also becoming a new emerging field that with no doubt will produce novel warped structures exhibiting interesting chiroptical properties.[59] Thus for instance, recent examples of graphene quantum dots with chiroptical properties[60] or the first nanographene with CPL properties[42] have been presented.

The possibility of preparing tailor-made defective curved carbon nanostructures might open up new pathways on carbon-based materials. The synthetic strategies shown here offer a fine control of the carbon nanostructures at the molecular level as required for their implementation in electronic devices.

Hence, we can envision innovative applications in different fields, such as in organic electronics, photovoltaics or sensing, by taking advantage of the curvatures and properties induced by the inclusion of defects in graphene-based materials.

Conflicts of interest

There are no conflicts to declare.

Acknowledgements

We acknowledge the European Research Council (ERC) under the European Union's Horizon 2020 research and innovation program (ERC-2015-STG-677023) and the Ministerio de Economía y Competitividad (MINECO, Spain) (CTQ2015-70283-P). A.G.C. and A. M. acknowledge contracts from MINECO (Spain) (RyC-2013-12943, IJCI-2016-27793).

Notes and references

1 (a) A. Hashimoto, K. Suenaga, A. Gloter, K. Urita and S. Iijima, *Nature*, 2004, **430**, 870–873; (b) J. C. Meyer, C. Kisielowski, R. Erni, M. D. Rossell, M. F. Crommie and A. Zettl, *Nano Lett.*, 2008, **8**, 3582–3586; (c) J. Lahiri, Y. Lin, P. Bozkurt, I. I. Oleynik and M. Batzill, *Nat. Nanotechnol.*, 2010, **5**, 326–329; (d) F. Banhart, J. Kotakoski and A. V. Krasheninnikov, *ACS Nano*, 2011, **5**, 26–41; (e) P. Y. Huang, C. S. Ruiz-Vargas, A. M. van der Zande, W. S. Whitney, M. P. Levendorf, J. W. Kevek, S. Garg, J. S. Alden, C. J. Hustedt, Y. Zhu, J. Park, P. L. McEuen and D. A. Muller, *Nature*, 2011, **469**, 389–392; (f) K. Kim, Z. Lee, W. Regan, C. Kisielowski, M. F. Crommie and A. Zettl, *ACS Nano*, 2011, **5**, 2142-2146; (g) S. Kurasch, J. Kotakoski, O. Lehtinen, V. Skákalová, J. Smet, C. E. Krill, A. V. Krasheninnikov and U. Kaiser, *Nano Lett.*, 2012, **12**, 3168–3173; (h) L. P. Biró and P. Lambin, *New J. Phys.*, 2013, **15**, 035024; (i) O. Lehtinen, N. Vats, G. Algara-Siller, P. Knyrim and U. Kaiser, *Nano Lett.*, 2015, **15**, 235–241; (j) S. T. Skowron, I. V. Lebedeva, A. M. Popov and E. Bichoutskaia, *Chem. Soc. Rev.*, 2015, **44**, 3143–3176.

2 (a) S. Iijima, T. Ichihashi and Y. Ando, *Nature*, 1992, **356**, 776–778; (b) A. W. Robertson, K. He, A. I. Kirkland and J. H. Warner, *Nano Lett.*, 2014, **14**, 908–914; (c) J. M. Leyssale and G. L. Vignoles, *J. Phys. Chem. C*, 2014, **118**, 8200–8216.

3 R. Rieger and K. Müllen, *J. Phys. Org. Chem.*, 2010, **23**, 315–325.

4 H. Terrones, R. Lv, M. Terrones and M. S. Dresselhaus, *Rep. Prog. Phys.*, 2012, **75**, 062501.

5 (a) F. Dötz, J. D. Brand, S. Ito, L. Gherghel and K. Müllen, *J. Am. Chem. Soc.*, 2000, **122**, 7707–7717; (b) Y. Segawa, H. Ito and K. Itami, *Nat. Rev. Mater.*, 2016, **1**, 15002.

6 (a) M. D. Watson, A. Fechtenkötter and K. Müllen, *Chem. Rev.*, 2001, **101**, 1267–1300; (b) J. Wu, W. Pisula and K. Müllen, *Chem. Rev.*, 2007, **107**, 718–747; (c) L. Chen, Y. Hernandez, X. Feng and K. Müllen, *Angew. Chem. Int. Ed.*, 2012, **51**, 7640–

7654; (d) A. Narita, X.-Y. Wang, X. Feng and K. Müllen, *Chem. Soc. Rev.*, 2015, **44**, 6616–6643; (e) A. Narita, X. Feng and K. Müllen, *Chem. Rec.*, 2015, **15**, 295–309.
7 (a) G. Otero, G. Biddau, C. Sánchez-Sánchez, R. Caillard, M. F. López, C. Rogero, F. J. Palomares, N. Cabello, M. A. Basanta, J. Ortega, J. Méndez, A. M. Echavarren, R. Pérez, B. Gómez-Lor and J. A. Martín-Gago, *Nature*, 2008, **454**, 865–868; (b) R. Dorel, P. de Mendoza, P. Calleja, S. Pascual, E. González-Cantalapiedra, N. Cabello and A. M. Echavarren, *Eur. J. Org. Chem.*, 2016, 3171–3176.
8 L. T. Scott, E. A. Jackson, Q. Zhang, B. D. Steinberg, M. Bancu and B. Li, *J. Am. Chem. Soc.*, 2012, **134**, 107–110.
9 (a) Y.-T. Wu and J. S. Siegel, *Chem. Rev.*, 2006, **106**, 4843–4867; (b) V. M. Tsefrikas and L. T. Scott, *Chem. Rev.*, 2006, **106**, 4868–4884.
10 T. Lenosky, X. Gonze, M. Teter and V. Elser, *Nature*, 1992, **355**, 333–335.
11 A. Eftekhari and H. Garcia, *Mat. Today Chem.*, 2017, **4**, 1–16.
12 (a) Q. Miao, *Chem. Rec.*, 2015, **15**, 1156–1159; (b) Q. Miao, *Polycyclic Arenes and Heteroarenes: Synthesis, Properties and Applications*, Wiley-VCH, Weinheim, 2016.
13 (a) A. Halleux, R. H. Martin and G. S. D. King, *Helv. Chim. Acta*, 1958, **42**, 1177–1183; (b) E. Clar, C. T. Ironside and M. Zander, *J. Chem. Soc.*, 1959, 142–147; (c) W. Hendel, Z. H. Khan and W. Schmidt, *Tetrahedron*, 1986, **42**, 1127–1134.
14 V. S. Iyer, M. Wehmeier, J. D. Brand, M. A. Keegstra and K. Müllen, *Angew. Chem. Int. Ed. Engl.*, 1997, **36**, 1604–1607.
15 (a) K. Mochida, K. Kawasumi, Y. Segawa and K. Itami, *J. Am. Chem. Soc.*, 2011, **133**, 10716–10719; (b) M. Grzybowski, K. Skonieczny, H. Butenschön and D. T. Gryko, *Angew. Chem. Int. Ed.*, 2013, **52**, 9900–9930; (b) T. Jin, J. Zhao, N. Asao and Y. Yamamoto, *Chem. Eur. J.*, 2014, **20**, 3554–3576; (c) Y. Segawa, T. Maekawa and K. Itami, *Angew. Chem. Int. Ed.*, 2015, **54**, 66–81; (d) K. Ozaki, K. Kawasumi, M. Shibata, H. Ito and K. Itami, *Nat. Commun.*, 2015, **6**:6251; (e) Y. Yano, H. Ito, Y. Segawa and K. Itami, *Synlett*, 2016, **27**, 2081–2084.
16 K. Müllen and X. Feng, *From Polyphenylenes to Nanographenes and Graphene Nanoribbons*, Springer Nature, Cham, 2017.
17 (a) K. Yamamoto, T. Harada, M. Nakazaki, T. Naka, Y. Kai, S. Harada and N. Kasai, *J. Am. Chem. Soc.*, 1983, **105**, 7171–7172; (b) K. Yamamoto, T. Harada, Y. Okamoto, H. Chikamatsu, M. Nakazaki, Y. Kai, T. Nakao, M. Tanaka, S. Harada and N. Kasai, *J. Am. Chem. Soc.*, 1988, **110**, 3578–3584.
18 (a) K. Yamamoto, Y. Saitho, D. Iwaki and T. Ooka, *Angew. Chem. Int. Ed. Engl.*, 1991, **30**, 1173–1174; (b) K. Yamamoto, *Pure Appl. Chem.*, 1993, **65**, 157–163.
19 K. Yamamoto, H. Sonobe, H. Matsubara, M. Sato, S. Okamoto and K. Kitaura, *Angew. Chem. Int. Ed. Engl.*, 1996, **35**, 69–70.
20 J. Luo, X. Xu, R. Mao and Q. Miao, *J. Am. Chem. Soc.*, 2012, **134**, 13796–13803.
21 L. Zhi and K. Müllen, *J. Mater. Chem.*, 2008, **18**, 1472–1484.
22 B. T. King, J. Kroulík, C. R. Robertson, P. Rempala, C. L. Hilton, J. D. Korinek and L. M. Gortari, *J. Org. Chem.*, 2007, **72**, 2279–2288.
23 E. U. Mughal and D. Kuck, *Chem. Commun.*, 2012, **48**, 8880–8882.
24 A. Pradhan, P. Dechambenoit, H. Bock and F. Durola, *J. Org. Chem.*, 2013, **78**, 2266–2274.
25 (a) K. Kawasumi, Q. Zhang, Y. Segawa, L. T. Scott and K. Itami, *Nat. Chem.*, 2013, **5**, 739–744; (b) K. Kato, Y. Segawa, L. T. Scott and K. Itami, *Chem. Asian J.*, 2015, **10**, 1635–1639.
26 K. Y. Cheung, X. Xu and Q. Miao, *J. Am. Chem. Soc.*, 2015, **137**, 3910–3914.
27 N. L. C. Leung, N. Xie, W. Yuan, Y. Liu, Q. Wu, Q. Peng, Q. Miao, J. W. Y. Lam and B. Z. Tang, *Chem. Eur. J.*, 2014, **20**, 15349–15353.
28 (a) H.-W. Ip, C.-F. Ng, H.-F. Chow and D. Kuck, *J. Am. Chem. Soc.*, 2016, **138**, 13778–13781. Other related examples: (b) E. U. Mughal, B. Neumann, H. G. Stammler and D. Kuck, *Eur. J. Org. Chem.*, 2014, 7469–7480; (c) H.-W. Ip, H.-F. Chow and D. Kuck, *Org. Chem. Front.*, 2017, **4**, 817–822; (d) W. S. Wong, C. F. Ng, D. Kuck and H. F. Chow, *Angew. Chem. Int. Ed.*, 2017, **56**, 12356–12360.
29 X. Gu, H. Li, B. Shan, Z. Liu and Q. Miao, *Org. Lett.*, 2017, **19**, 2246–2249.
30 T. Fujikawa, Y. Segawa and K. Itami, *J. Am. Chem. Soc.*, 2015, **137**, 7763–7768.
31 T. Fujikawa, Y. Segawa and K. Itami, *J. Org. Chem.*, 2017, **82**, 7745–7749.
32 (a) K. Shiraishi, A. Rajca, M. Pink and S. Rajca, *J. Am. Chem. Soc.*, 2005, **127**, 9312–9313; (b) T. Fujikawa, D. V. Preda, Y. Segawa, K. Itami and L. T. Scott, *Org. Lett.*, 2016, **18**, 3992–3995; (c) V. Rajeshkumar and M. C. Stuparu, *Chem. Commun.*, 2016, **52**, 9957–9960; (d) N. J. Schuster, D. W. Paley, S. Jockusch, F. Ng, M. L. Steigerwald and C. Nuckolls, *Angew. Chem. Int. Ed.*, 2016, **55**, 13519–13523; (e) X.-Y. Wang, X.-C. Wang, A. Narita, M. Wagner, X.-Y. Cao, X. Feng and K. Müllen, *J. Am. Chem. Soc.*, 2016, **138**, 12783–12786.
33 N. Fukui, T. Kim, D. Kim and A. Osuka, *J. Am. Chem. Soc.*, 2017, **139**, 9075–9088.
34 (a) X. Dou, X. Yang, G. J. Bodwell, M. Wagner, V. Enkelmann and K. Müllen, *Org. Lett.*, 2007, **9**, 2485–2488; (b) J. L. Ormsby, T. D. Black, C. L. Hilton, Bharat and B. T. King, *Tetrahedron*, 2008, **64**, 11370–11378.
35 S. Nobusue, K. Fujita and Y. Tobe, *Org. Lett.*, 2017, **19**, 3227–3230.
36 I. R. Márquez, N. Fuentes, C. M. Cruz, V. Puente-Muñoz, L. Sotorrios, M. L. Marcos, D. Choquesillo-Lazarte, B. Biel, L. Crovetto, E. Gómez-Bengoa, M. T. González, R. Martin, J. M. Cuerva and A. G. Campaña, *Chem. Sci.*, 2017, **8**, 1068–1074.
37 Reviews on Ni-catalyzed cross-coupling reactions: (a) J. Cornella, C. Zarate and R. Martin, *Chem. Soc. Rev.*, 2014, **43**, 8081–8097; (b) M. Tobisu and N. Chatani, *Acc. Chem. Res.*, 2015, **48**, 1717–1726; (c) B. Su, Z.-C. Cao and Z.-J. Shi, *Acc. Chem. Res.*, 2015, **48**, 886–896. Other selected examples: (d) E. Wenkert, E. L. Michelotti and C. S. Swindell, *J. Am. Chem. Soc.*, 1979, **101**, 2246–2247; (e) E. Wenkert, E. L. Michelotti, C. S. Swindell and M. Tingoli, *J. Org. Chem.*, 1984, **49**, 4894–4899; (f) J. W. Dankwardt, *Angew. Chem. Int. Ed.*, 2004, **43**, 2428–2432; (g) B.-T. Guan, S.-K. Xiang, T. Wu, Z.-P. Sun, B.-Q. Wang, K.-Q. Zhao and Z.-J. Shi, *Chem. Commun.*, 2008, 1437–1439; (h) J. Cornella and M. Ruben, *Org. Lett.*, 2013, **15**, 6298–6301; (i) M. Tobisu, T. Takahira and N. Chatani, *Org. Lett.*, 2015, **17**, 4352–4355.
38 F. Würthner, *Chem. Commun.*, 2004, 1564–1579.
39 (a) Z. Sun, Q. Ye, C. Chi and J. Wu, *Chem. Soc. Rev.*, 2012, **41**, 7857–7889; (b) T. Dumslaff, B. Yang, A. Maghsoumi, G. Velpula, K. S. Mali, C. Castiglioni, S. De Feyter, M. Tommasini, A. Narita, X. Feng and K. Müllen, *J. Am. Chem. Soc.*, 2016, **138**, 4726–4729.
40 V. G. Jiménez, R. Tapia, M. A. Medel, I. F. A. Mariz, T. Ribeiro, V. Blanco, J. M. Cuerva, E. Maçôas and A. G. Campaña, *Chem. Commun.*, 2018, DOI: 10.1039/C8CC00386F.
41 J. Luo, K. Song, F. l. Gu and Q. Miao, *Chem. Sci.*, 2011, **2**, 2029–2034.
42 C. M. Cruz, I. R. Márquez, I. F. A. Mariz, V. Blanco, C. Sánchez-Sánchez, J. M. Sobrado, J. A. Martín-Gago, J. M. Cuerva, E. Maçôas and A. G. Campaña, *Chem. Sci.*, 2018, DOI: 10.1039/C8SC00427G.
43 Reviews on CPL: (a) E. M. Sánchez-Carnerero, A. R. Agarrabeitia, F. Moreno, B. L. Maroto, G. Muller, M. J. Ortiz and S. de la Moya, *Chem. Eur. J.*, 2015, **21**, 13488–13500; (b) J. Kumar, T. Nakashima and T. Kawai, *J. Phys. Chem. Lett.*,

2015, **6**, 3445–3452; (c) G. Longhi, E. Castiglioni, J. Koshoubu, G. Mazzeo and S. Abbate, *Chirality*, 2016, **28**, 696–707.
44 Selected recent examples of helicene-based CPL-active compounds: (a) K. Nakamura, S. Furumi, M. Takeuchi, T. Shibuya and K. Tanaka, *J. Am. Chem. Soc.*, 2014, **136**, 5555–5558; (b) N. Saleh, M. Srebro, T. Reynaldo, N. Vanthuyne, L. Toupet, V. Y. Chang, G. Muller, J. A. G. Williams, C. Roussel, J. Autschbach and J. Crassous, *Chem. Commun.*, 2015, **51**, 3754–3757; (c) T. Matsuno, Y. Koyama, S. Hiroto, J. Kumar, T. Kawai and H. Shinokubo, *Chem. Commun.*, 2015, **51**, 4607–4610; (d) I. H. Delgado, S. Pascal, A. Wallabregue, R. Duwald, C. Besnard, L. Guénée, C. Nançoz, E. Vauthey, R. C. Tovar, J. L. Lunkley, G. Muller and J. Lacour, *Chem. Sci.*, 2016, **7**, 4685–4693; (e) N. Hellou, M. Srebro-Hooper, L. Favereau, F. Zinna, E. Caytan, L. Toupet, V. Dorcet, M. Jean, N. Vanthuyne, J. A. G. Williams, L. Di Bari, J. Autschbach and J. Crassous, *Angew. Chem. Int. Ed.*, 2017, **56**, 8236–8239; (f) H. Nishimura, K. Tanaka, Y. Morisaki, Y. Chujo, A. Wakamiya and Y. Murata, *J. Org. Chem.*, 2017, **82**, 5242–5249; (g) K. Dhbaibi, L. Favereau, M. Srebro-Hooper, M. Jean, N. Vanthuyne, F. Zinna, B. Jamoussi, L. Di Bari, J. Autschbach and J. Crassous, *Chem. Sci.*, 2018, **9**, 735–742; (h) A. U. Malik, F. Gan, C. Shen, N. Yu, R. Wang, J. Crassous, M. Shu and H. Qiu, *J. Am. Chem. Soc.*, 2018, **140**, 2769–2772.
45 P. Ravat, R. Hinkelmann, D. Steinebrunner, A. Prescimone, I. Bodoky and M. Juríček, *Org. Lett.*, 2017, **19**, 3707–3710.
46 Selected helical π-extended PAHs: (a) D. Peña, D. Pérez, E. Guitián and L. Castedo, *Org. Lett.*, 1999, **1**, 1555–1557; (b) X. Geng, J. P. Donahue, J. T. Mague and R. A. Pascal, *Angew. Chem. Int. Ed.*, 2015, **54**, 13957–13960; (c) Y. Zhong, T. J. Sisto, B. Zhang, K. Miyata, X.-Y. Zhu, M. L. Steigerwald, F. Ng and C. Nuckolls, *J. Am. Chem. Soc.*, 2017, **139**, 5644–5647; (d) M. Daigle, D. Miao, A. Lucotti, M. Tommasini and J. F. Morin, *Angew. Chem. Int. Ed.*, 2017, **56**, 6213–6217; (e) W. Yang, G. Longhi, S. Abbate, A. Lucotti, M. Tommasini, C. Villani, V. J. Catalano, A. O. Lykhin, S. A. Varganov and W. A. Chalifoux, *J. Am. Chem. Soc.*, 2017, **139**, 13102–13109; (f) V. Berezhnaia, M. Roy, N. Vanthuyne, M. Villa, J. V. Naubron, J. Rodriguez, Y. Coquerel and M. Gingras, *J. Am. Chem. Soc.*, 2017, **139**, 18508–18511; (g) T. Hosokawa, Y. Takahashi, T. Matsushima, S. Watanabe, S. Kikkawa, I. Azumaya, A. Tsurusaki and K. Kamikawa, *J. Am. Chem. Soc.*, 2017, **139**, 18512–18521; (h) P. J. Evans, J. Ouyang, L. Favereau, J. Crassous, I. Fernández, J. Perles Hernáez and N. Martín, *Angew. Chem. Int. Ed.*, 2018, DOI: 10.1002/anie.201800798; (i) Y. Zhu, Z. Xia, Z. Cai, Z. Yuan, N. Jiang, T. Li, Y. Wang, X. Guo, Z. Li, S. Ma, D. Zhong, Y. Li and J. Wang, *J. Am. Chem. Soc.*, 2018, DOI: 10.1021/jacs.8b01447; (j) Y. Nakakuki, T. Hirose, H. Sotome, H. Miyasaka and K. Matsuda, *J. Am. Chem. Soc.*, 2018, DOI: 10.1021/jacs.7b13412.
47 S. H. Pun, C. K. Chan, J. Luo, Z. Liu and Q. Miao, *Angew. Chem. Int. Ed.*, 2018, **57**, 1581–1586.
48 J. Bordner, R. G. Parker and R. H. Stanford, *Acta Cryst., B.* 1972, **B28**, 1069–1075.
49 B. Thulin and O. Wennerström, *Acta Chem. Scand. B*, 1976, **30**, 369–371.
50 C.-N. Feng, M.-Y. Kuo and Y.-T. Wu, *Angew. Chem. Int. Ed.*, 2013, **52**, 7791–7794.
51 Y. Sakamoto and T. Suzuki, *J. Am. Chem. Soc.*, 2013, **135**, 14074–14077.
52 R. W. Miller, A. K. Duncan, S. T. Schneebeli, D. L. Gray and A. C. Whalley, *Chem. Eur. J.*, 2014, **20**, 3705–3711.
53 R. W. Miller, S. E. Averill, S. J. Van Wyck and A. C. Whalley, *J. Org. Chem.*, 2016, **81**, 12001–12005.
54 S. Nobusue and Y. Tobe, *Synlett*, 2016, **27**, 2140–2144.
55 K. Y. Cheung, C. K. Chan, Z. Liu and Q. Miao, *Angew. Chem. Int. Ed.*, 2017, **56**, 9003–9007.
56 J. Mei, N. L. C. Leung, R. T. K. Kwok, J. W. Y. Lam and B. Z. Tang, *Chem. Rev.*, 2015, **115**, 11718–11940.
57 U. Beser, M. Kastler, A. Maghsoumi, M. Wagner, C. Castiglioni, M. Tommasini, A. Narita, X. Feng and K. Müllen, *J. Am. Chem. Soc.*, 2016, **138**, 4322–4325.
58 M. Stępień, E. Gońka, M. Żyła and N. Sprutta, *Chem. Rev.*, 2017, **117**, 3479–3716.
59 M. Rickhaus, M. Mayor and M. Juríček, *Chem. Soc. Rev.*, 2017, **46**, 1643–1660.
60 (a) N. Suzuki, Y. Wang, P. Elvati, Z.-B. Qu, K. Kim, S. Jiang, E. Baumeister, J. Lee, B. Yeom, J. H. Bahng, J. Lee, A. Violi and N. A. Kotov, *ACS Nano*, 2016, **10**, 1744–1755; (b) M. Vázquez-Nakagawa, L. Rodríguez-Pérez, M. A. Herranz and N. Martín, *Chem. Commun.*, 2016, **52**, 665–668.

